Identification of arachidonate epoxides/diols by capillary chromatography–mass spectrometry

Mike VanRollins[1] **and Howard R. Knapp**

Division of Clinical Pharmacology, Department of Internal Medicine, University of Iowa, Iowa City, IA 52242

Abstract The identification of epoxide regioisomers of arachidonic acid (EETs) as methyl esters is difficult because they coelute during gas chromatography and possess similar mass spectra. In the present study, EETs and their hydrolysis products, dihydroxyeicosatrienoic acids (DHETs), were analyzed as pentafluorobenzyl ester derivatives and their properties were compared to other esters. The four EET regioisomers were not resolved by gas chromatography as pentafluorobenzyl, trimethylsilyl, *t*-butyldimethylsilyl, or methyl esters. However, after being hydrolyzed to DHETs, three of the four regioisomers were resolved as (*bis*)-*t*-butyldimethylsilyl ether, pentafluorobenzyl esters. The fourth regioisomer (5,6-DHET) was resolved after being converted to a δ-lactone. Thus, the EETs could be resolved by capillary gas chromatography once converted to DHETs. Pentafluorobenzyl esters of both EETs and DHETs (15–40 ng) provided diagnostic spectra when analyzed by electron ionization mass spectrometry. The mass spectral interpretations that indicated epoxide and diol positions were validated using synthesized EET/DHET [17,17,18,18-d_4, 5,6,8,9,11,12,14,15 d_8] standards. Lesser amounts of DHETs (5–150 fg) also indicated molecular weights when analyzed in the negative-ion chemical-ionization mode. In summary, EETs in nanogram quantities were identified as pentafluorobenzyl esters using electron ionization mass spectrometry. EETs in femtogram-to-picogram quantities were also identified after conversion to DHETs and analysis by gas chromatography–mass spectrometry in the negative ion-chemical ionization mode.—**VanRollins, M., and H. R. Knapp.** Identification of arachidonate epoxides/diols by capillary chromatography–mass spectrometry. *J. Lipid Res.* 1995. **36:** 952–966.

Supplementary key words arachidonic acid • polyunsaturated fatty acids • eicosanoids • epoxyeicosatrienoic acids • dihydroxyeicosatrienoic acid

The metabolism of arachidonic acid by cytochrome P450 monooxygenases results in three types of products: epoxyeicosatrienoic acids (14,15-, 11,12-, 8,9-, and 5,6-EETs); 20- and 19-hydroxyarachidonic acid; and *cis-trans* conjugated hydroxyeicosatetraenoic acids such as 12-(R)-HETE (1, 2). To date, only the EETs have been reported to occur in plasma: 1.0 nM as unesterified acids, and 300 nM as phospholipid esters in lipoproteins (3). The EETs in solid tissues also occur primarily esterified to phospholipids (4). A sensitive method to identify small amounts of endogenous EETs is thus critical to establish the presence of these eicosanoids in tissues.

To analyze EETs by gas chromatography–mass spectrometry (GC–MS), the four regioisomers must first be isolated by reversed-phase and normal-phase HPLC because they are poorly resolved by capillary GC, at least as methyl or pentafluorobenzyl esters (5, 6). Due to the low sensitivity of UV detection and adsorptive losses, standard HPLC techniques require μg amounts of EETs and other fatty epoxides (7, 8). Once isolated, ng amounts of EETs can be used to establish the molecular weights when pentafluorobenzyl esters are analyzed by GC–MS in the negative ion-chemical ionization (NICI) mode (6). However, due to a lack of chromatographic resolution, this GC–MS approach does not differentiate between individual isomers possessing the same molecular ion. Likewise, GC–MS studies on EET methyl esters using conventional electron ionization techniques do not readily differentiate the regioisomers because the ions indicating the position of the oxirane ring occur at low masses and/or are weak in intensity (<3%) (9). When the methyl esters are ionized by $CS_2^{+\cdot}$, one fragment (150–220 *m/z*) is intensified that characterizes the oxirane ring position (10). Unfortunately, the amount of EET required for this novel ionization technique is unknown. In contrast to methyl esters, use of the picolinyl esters of EETs and conventional electron ionization techniques results in spectra that are readily diagnostic, i.e., identify the oxirane ring position with ions of moderate mass and intensity (11). However,

Abbreviations: EET, epoxyeicosatrienoic acid; DHET, dihydroxyeicosatrienoic acid; HPLC, high performance liquid chromatography; GC–MS, gas chromatography–mass spectrometry; NICI, electron capture negative chemical ionization; ECL, equivalent chain length.

[1]To whom reprint requests should be addressed at: Division of Clinical Pharmacology, Department of Internal Medicine, C31-O GH, University of Iowa, Iowa City, IA 52242.

in our hands this technique lacks reproducibility unless μg quantities are derivatized (8). In the present report, a method to identify EETs in fg to pg quantities is described.

EXPERIMENTAL

Derivatization

Deuterated arachidonic acids [17,17,18,18-d_4 and 5,6,8,9,11,12,14,15-d_8] were purchased from Medical Isotopes (Concord, NH) or were a generous gift from Mr. Eric Petty (Vanderbilt University). EET standards were purchased from Cayman Chemical Co. (Ann Arbor, MI) or synthesized using standard methods (7, 8). DHETs were prepared by acid-catalyzed hydrolysis of EETs with yields ranging from 63- to 94% (8). Catalytic hydrogenation was done as before using 5% Rh on Al_2O_3 to minimize hydrogenolysis (12). Methyl, trimethylsilyl, *t*-butyldimethylsilyl, and pentafluorobenzyl esters were prepared by standard methods (6, 13, 14). Diazomethane was synthesized using a macro-generator (Aldrich Chemical Co., Milwaukee, WI). The *t*-butyldimethylsilyl chloride, N-methyl-N-trimethylsilyltrifluoroacetamide, and 1% *t*-butyldimethylsilylimidazole in dimethylformamide were purchased from Aldrich Chemical Co., Pierce Chemical Co. (Rockford, IL), and Supelco (Bellefonte, PA), respectively. All solvents used were Optima grade (Fisher Chemical Co.).

Capillary gas chromatography and mass spectrometry

EET and DHET derivatives were examined using two Hewlett-Packard quadrupole systems: models 5970B (MSD) and 5989A (Engine). Studies of various ester types were done with the 5970B interfaced to a 5980 GC with on-column injector (J&W, Rancho Cordova, CA). Samples were dissolved in 1.0 μl isooctane or tridecane and injected into a wall-coated (0.25 μm film of dimethylpolysiloxane; DB-1, J&W), fused-silica column [0.25 mm (i.d.) × 28 m]. The linear velocity of carrier gas (99.9999% helium) was 25 cm/sec with the oven at 230°C. One min after injection, the oven temperature was ramped 70°C/min from 90°C (isooctane) or 225°C (tridecane) to a final constant temperature. The transfer line was maintained at 5°C above final oven temperatures.

A Hewlett-Packard 5989A, interfaced to a 5980 GC (Series II) with on-column ("duckbill") injector and programmable flow rates, was used for analysis of pentafluorobenzyl ester derivatives. The temperatures of the ion source and the analyzer were 200°C and 100°C, respectively. Electron ionization experiments (70 eV) were carried out using a linear velocity of 60 cm/sec, and a DB-1 column (0.25 mm (i.d.) × 6 m with a 0.25 μm thick film). Negative ion-chemical ionization (230 eV) studies (NICI) were done using methane at 1.6 torr. Samples were dissolved in 1.0 μl isooctane and injected into a wall-coated (0.25 μm film of 5% diphenyldimethylpolysiloxane; DB5-MS, J&W), fused-silica column [0.25 mm (i.d.)]. For optimal sensitivity, a 15-m column with helium flowing at 90 cm/sec was used; 1.0 min after injection, the oven temperature was ramped from 90°C at 30°C/min to 280°C. For optimal resolution, a 60-m column with helium flowing at 24 cm/sec was used; 1.0 min after injection, the oven temperature was ramped from 230°C at 70°C/min to 300°C.

To characterize the retention times of various derivatives, a plot of carbon number versus log (retention time) was generated using 20:0, 21:0, 22:0, 23:0, 24:0, 25:0, 26:0, and 27:0 as methyl, trimethylsilyl, *t*-butyldimethylsilyl, and pentafluorobenzyl esters. Individual equivalent chain length (ECL) values were determined from the interpolated $\log_{10}$ (retention times).

Signal-to-noise measurements (root mean square) were performed using the Hewlett-Packard software.

RESULTS AND DISCUSSION

Gas chromatographic properties

EETs. The ECLs of the pentafluorobenzyl esters of the four EET regioisomers ranged from 20.47 to 20.57, which

TABLE 1. The equivalent chain lengths (ECL) of DHETs as determined by capillary gas chromatography

Regioisomer	(*bis*)Trimethylsilyl Ether, Methyl Ester[a]	(*bis*)Trimethylsilyl Ether, Trimethylsilyl Ester[b]	(*bis*)Trimethylsilyl Ether, Pentafluorobenzyl Ester[c]	(*bis*)-*t*-Butyldimethylsilyl Ether, Methyl Ester[a]	(*bis*)-*t*-Butyldimethylsilyl Ether, *t*-Butyldimethylsilyl Ester[d]	(*bis*)-*t*-Butyldimethylsilyl Ether, Pentafluorobenzyl Ester[c]
14,15-DHET	22.72	22.59	22.37	26.96	26.85	26.80
11,12-DHET	22.54	22.40	22.19	26.75	26.59	26.55
8,9-DHET	22.54	22.38	22.16	26.76	26.49	26.49
5,6-DHET	22.65 (22.92)[f]	22.46 (21.85)[f]	22.21 (18.17)[f]	26.86 (23.14)[g]	26.49 (19.42)[g]	26.44 (18.61)[g]

[a–c]Various derivatives of synthetic DHETs were injected onto a non-polar column, and eluted isothermally at 250°[a],260°[b], 280°[c], 290°[d], and 295°C[e],respectively. A plot of carbon number versus log (retention time) was generated using fatty acid standards of the same ester type, and ECL values were determined from the interpolated log (retention times).

[f]The value in parentheses is for the 6-trimethylsilyl-5-lactone and is relative to fatty acid standards as methyl, trimethylsilyl, and pentafluorobenzyl esters.

[g]The value in parentheses is for the 6-*t*-butyldimethylsilyl-5-lactone and is relative to fatty acid standards as methyl, *t*-butyldimethylsilyl, and pentafluorobenzyl esters.

were distinctly less than the methyl (20.89–20.93); trimethylsilyl (20.85–21.76), and *t*-butyldimethylsilyl (20.85–21.06) esters. Thus, determination of the ECL of pentfluorobenzyl and methyl ester derivatives permits a chromatographic identification of EETs as a group. Hydrogenation increased the EET retention times, e.g., to 21.52–21.65 for the methyl esters. Yet, hydrogenation yielded little improvement in the separation of individual EETs. Thus, the use of pentafluorobenzyl and methyl esters permits only the chromatographic identification of EETs as a group. However, the ECLs of regioisomers are too close to differentiate individual EETs.

DHETs. The diol regioisomers were better resolved than the parent epoxides. The retention times of various ester derivatives were greatest when the vicinal diol occurred close to either end of the molecule (**Table 1**). This effect of diol position was most pronounced in the methyl ester series, and was true whether the diols were derivatized as trimethylsilyl or *t*-butyldimethylsilyl ethers. The difficult to separate 8,9-DHET and 11,12-DHET were nearly baseline-resolved when derivatized as the *t*-butyldimethylsilyl ether, pentafluorobenzyl esters (**Fig. 1,** Table 1). Thus, three of the four DHETs could be resolved by capillary GC after conversion to *t*-butyldimethylsilyl ether, pentafluorobenzyl esters.

Whether 5,6-DHET and 5,6-EET occur in vivo is uncertain, largely due to technical difficulties in their analyses (15). When biological samples are concentrated at pH 7.4, 5,6-DHET acid-catalyzes its own lactonization with formation of a stable, six-membered ring (6). Moreover, when derivatized for 16 h at 25°C under basic conditions [N-methyl-N-trimethylsilyl-trifluoroacetamide and pyridine (13)], at least 5–10% of 5,6-DHET is converted to a δ-lactone (data not shown). Once the C_6 hydroxy group is silylated, the 6-silylether, 1,5-lactone product elutes before the external ester (Table 1, bottom row). The one exception to this elution pattern is the 6-trimethylsilylether, 1,5-lactone which comes after the corresponding (*bis*)trimethylsilylether, methyl ester. In each series described in Table 1, the 5,6-DHET lactone was readily resolved from the other DHET regioisomers. Thus, pretreating 5,6-DHET with acid and trimethylsilylation of the resulting product permitted the chromatographic identification of 5,6-DHET.

Like 5,6-DHET, 5,6-EET also spontaneously forms 6-hydroxy-1,5-lactone and this conversion is catalyzed by acid; less than 10% of 5,6-EET remains intact when incubated 4 h at 25°C in the presence of dilute aqueous acid (data not shown). Upon silylation and capillary gas chromatography, the 1,5-lactone is readily resolved from external esters of DHET (Table 1). Depending upon the type of silyl moiety at C_6, the δ-lactone elutes either before (6-*t*-butyldimethylsilylether-1,5-lactone) or after (6-trimethylsilylether-1,5-lactone) the corresponding 5,6-EET ester. Perhaps more importantly, either 1,5-lactone derivative is readily resolved from the other three EET regioisomers (Table 1). Thus, treating 5,6-EET with acid and forming a 6-*t*-butyltrimethylsilylether-1,5-lactone allows the chromatographic identification of 5,6-EET. Because, under these same conditions, the other three EET regioisomers form DHETs that can be converted to pentafluorobenzyl-esters and separated by gas chromatography (Fig. 1), all four EET regioisomers may be chromatographically identified once converted to *t*-butyldimethylsilyl ethers.

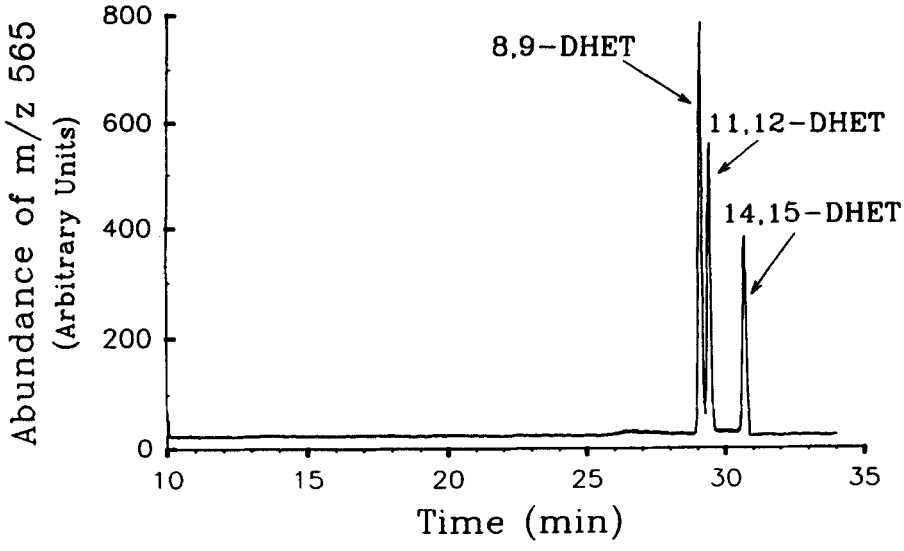

Fig. 1. Gas chromatography of DHET regioisomers. DHETs (82 pg each) were converted to a (*bis*)-*t*-butyldimethylsilyl ether, pentafluorobenzyl ester, injected into a 60 m non-polar column, and chromatographed isothermally at 300°C. The *m/z* 565 ($M-C_6F_5CH_2$) was monitored in the negative-ion, chemical (CH_4) ionization mode.

Mass spectral properties of EETs and DHETs as lactones (internal esters)

As noted above, both 5,6-DHET and 5,6-EET were converted by acid-catalyzed hydrolysis to a common product, the 6-hydroxy-1,5-lactone. For further identification, the lactone product was silylated, gas chromatographed, and subjected to electron ionization mass spectrometry. The electron ionization spectrum of 6-*t*-butyldimethylsilyl ether-1,5-lactone was diagnostic (**Fig. 2A**) and readily interpretable. A molecular weight of 434 was established by multiple fragments: *m/z* 434 (M), 419 (M-CH_3), 377 (M-C[CH_3]$_3$), and 359 (M-[C[CH_3]$_3$ + H_2O]). The molecular weight plus prominent ions like *m/z* 73 ([CH_3]$_3$Si), 75 (HOSi[CH_3]$_2$), and 131

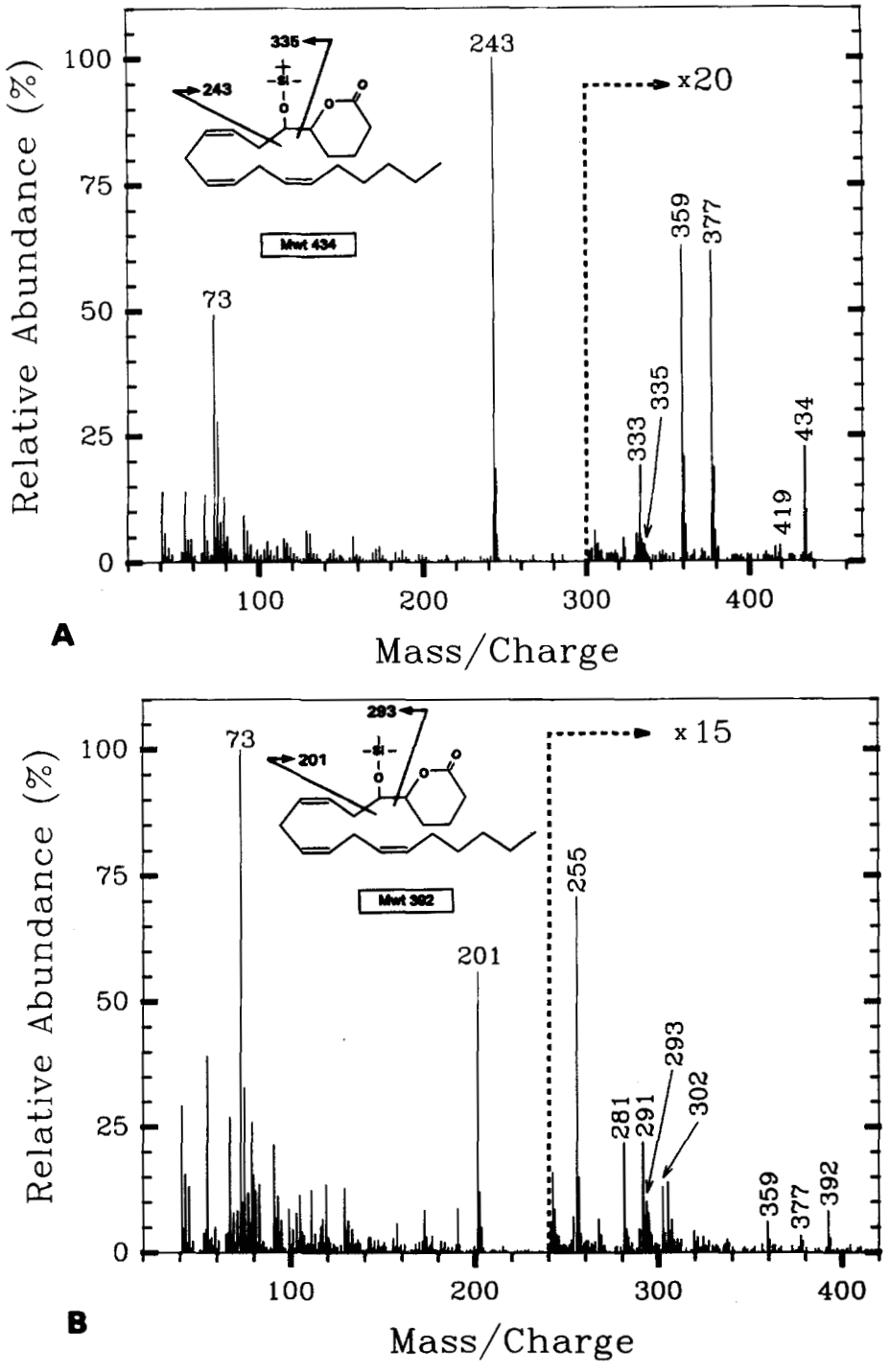

Fig. 2. Electron ionization (70 eV) mass spectra of (A) 6-*t*-butyldimethylsilyl- and (B) 6-trimethylsilyl- 1,5-lactones of 5,6-DHET.

$(OSi[CH_3]_2C[CH_3]_3)$ indicated that a single *t*-butyldimethylsilyl moiety had been added to the lactone (16). Fragments 335 ($CH_3[CH_2]_4[CH{=}CHCH_2]_3CHOSi[CH_3]_2C[CH_3]_3$), 333 ($CH_3[CH_2]_4[CH{=}CHCH_2]_3CHOSi[CH_3]_2C[CH_3]_3-H_2$), and 243 ($M-CH_3[CH_2]_4[CH{=}CHCH_2]_3$) also indicated that the $OSi[CH_3]_2C[CH_3]_3$ was in ether linkage at C_6. The intensity of the 243 fragment was much greater than that of *m/z* 335, probably because of two factors: a loss of two hydrogen atoms at C_6 and C_7 from *m/z* 335 generated a stable conjugated diene byproduct (*m/z* 333), and *m/z* 243 delocalized the positive charge over three oxygen atoms while *m/z* 293 and 291 only localized the charge over a single oxygen (12). Because of such intense fragments, the spectra of the 6-*t*-butyldimethylsilylated, 1,5-lactone was strikingly different from that of other EET and DHET regioisomers (see below).

The electron ionization spectrum of 6-trimethylsilylether-1,5-lactone was also diagnostic (Fig. 2B) and readily interpretable. A molecular weight of 392 was indicated by *m/z* 392 (M), 377 ($M-CH_3$), 359 ($M-[CH_3 + H_2O]$), 305 ($M-CH_3[CH_2]_4CH{=}CHCH_2$), 302 ($M-[CH_3]_3SiOH$), 281 ($M-CH_3(CH_2)_4CH{=}CHCH_2$), and 255 ($M-CH_3[CH_2]_4CH{=}CH_2CH_2CH{=}CH$) (16). Likewise, the presence of a single trimethylsilyl group was indicated by a prominent *m/z* 73 ($[CH_3]_3Si$) and weaker *m/z* 75 ($HOSi[CH_3]_2$), 103 ($CH_2{=}OSi[CH_3]_3$), 117

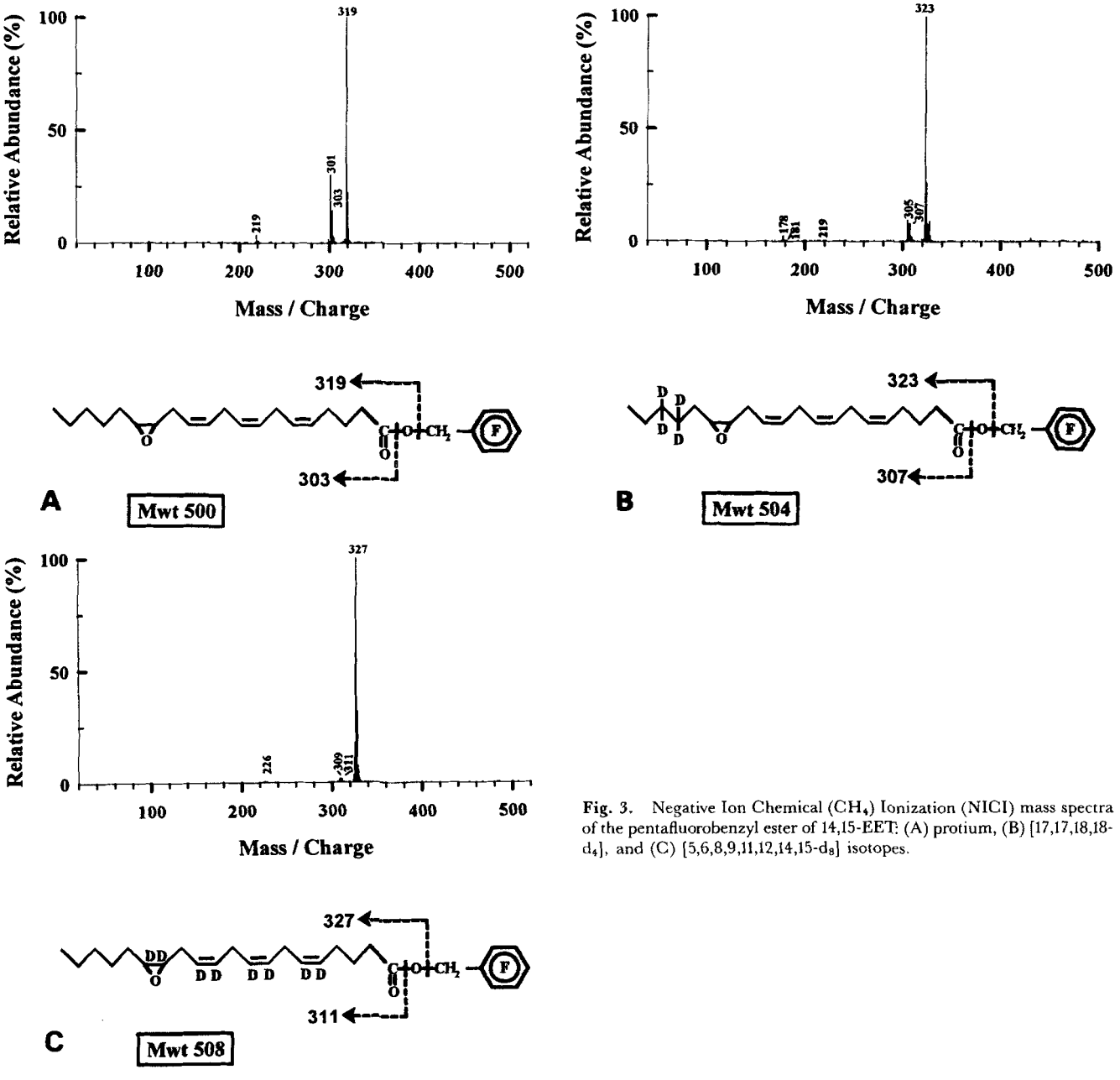

Fig. 3. Negative Ion Chemical (CH_4) Ionization (NICI) mass spectra of the pentafluorobenzyl ester of 14,15-EET: (A) protium, (B) [17,17,18,18-d_4], and (C) [5,6,8,9,11,12,14,15-d_8] isotopes.

($CH_2CH_2OSi[CH_3]_3$), and 129 ($CH_2{=}CHCH_2OSi[CH_3]_3$). The trimethylsilyl group was bound to C_6 in ether linkage, as suggested by *m/z* 293 ($CH_3[CH_2]_4[CH{=}CHCH_2]_3CHOSi[CH_3]_3$), 291 ($CH_3[CH_2]_4[CH{=}CHCH_2]_3CHOSi[CH_3]_3$-$H_2$), and 201 (M-$CH_3[CH_2]_4[CH{=}CHCH_2]_3$). The intensity of the α fragment 201 was much greater than that of *m/z* 293, probably because of the same two factors discussed above: *m/z* 201 having more capacity than *m/z* 293 and 291 to delocalize the positive charge, and the formation of *m/z* 291 at the expense of 293 (12). In summary, both the chromatographic properties and the electron ionization spectra of the 5,6-EET

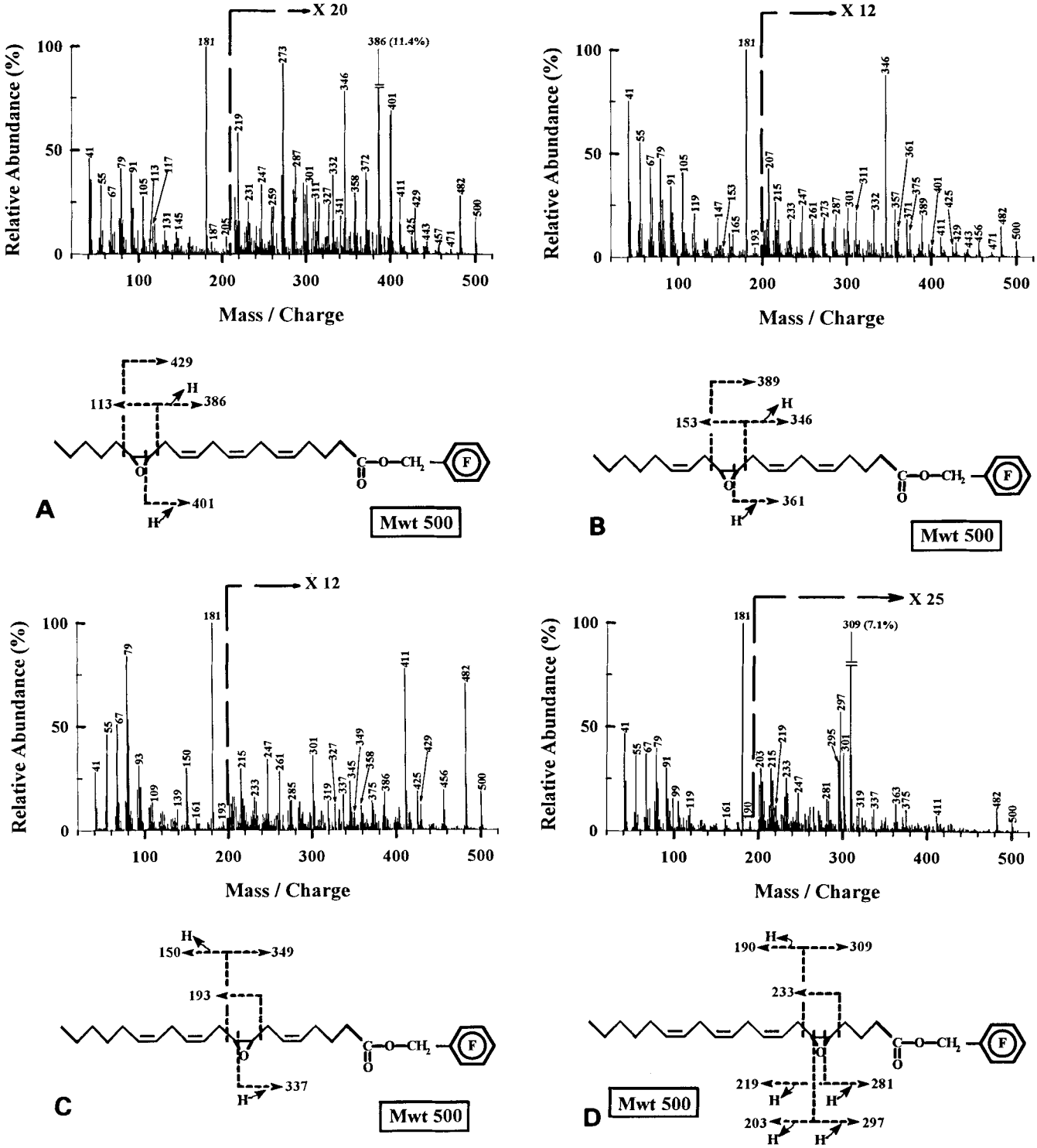

Fig. 4. Electron ionization mass spectra of the pentafluorobenzylester of (A) 14,15-, (B) 11,12-, (C) 8,9-, and (D) 5,6-EET.

and 5,6-DHET δ-lactones are characteristic, and readily differentiated from the other EET and DHET regioisomers. Absent in the 5-HETE δ-lactone (16), the presence of a silyl group at C_6 directs the major cleavage to occur between C_6 and C_7.

Mass spectral properties of EETs and DHETs as pentafluorobenzyl esters: NICI spectra of EET-pentafluorobenzyl esters

An important consideration in metabolite identification is the minimum amount of sample required for mass spectral identification. To determine this limit, standards were injected in decreasing amounts until the relative intensities of diagnostic ions changed by more than 15%. Under our experimental conditions, the proportions of major diagnostic ions were altered before diagnostic ions of ca. 2–3% relative intensity disappeared from the spectrum, i.e., the weaker diagnostic ions became less than 3 times the background intensity. At this minimum concentration, the signal-to-noise level for the summed ions (total ion current) was recorded for correlative purposes.

The NICI spectra of the four EETs resembled published results (6, 17–19). Moreover, 20 pg of each EET was enough to duplicate the relative intensities of *m/z* 319, 303 and 301 generated with 200 ng EET. At 20 pg, the total ion current produced a signal-to-noise ratio of 29 ± 8 to 1.0. The spectra from 14,15-, 11,12-, and 8,9-EET regioisomers contained the following fragments in common: 482 ($M-H_2O$; 0.0–0.1% relative intensity), 480 ($M-[H_2O+H_2]$; 0.0–0.1%), 319 ($M-CH_2C_6F_5$; 100%), 303 ($M-OCH_2C_6F_5$; 8.2–13.8%), and 301 ($M-[CH_2C_6F_5+H_2O]$; 13.6–29.0%) (**Fig. 3A**). To validate the spectral interpretations, synthetic deuterated DHET standards were studied. As predicted, the masses of *m/z* 480 (or 482), 319, 303, and 301 increased by 4 daltons when EETs[17,17,18,18-d_4] were examined (Fig. 3B). Likewise, *m/z* 319 and 303 increased by 8 daltons in the spectra of all EETs[5,6,8,9,11,12,14,15-d_8] (Fig. 3C). However, depending upon the regioisomer, varying amounts of HDO were lost, and the *m/z* 301 and 480 fragments would increase by only 7 daltons instead of 8 daltons (Fig. 3C). Together, these mass shifts validated the spectral interpretations, and confirmed a common molecular weight of 500 for all four EET regioisomers. A molecular weight of 500 was also evident when 150 fg was injected and only *m/z* 319 was monitored; at this level of injectate, the signal-to-noise of the total ion peak was 31 ± 5 to 1.0.

Electron ionization spectra of EET-pentafluorobenzyl esters

Pentafluorobenzyl esters of eicosanoids are normally examined in the NICI mode because of high sensitivity, and because the ($M-CH_2C_6F_5$) fragment tends to be the base peak (see above). We tested whether pentafluorobenzyl esters provide additional structural information when subjected to electron ionization by conventional techniques, as done earlier for 5-HETE (20). Unlike the NICI spectra, the electron ionization spectra were diagnostic, that is, standards of the four EETs could be differentiated (**Fig. 4**). All the spectra contained ions that identified the 500 molecular weight: *m/z* 500 (M; 0.2–

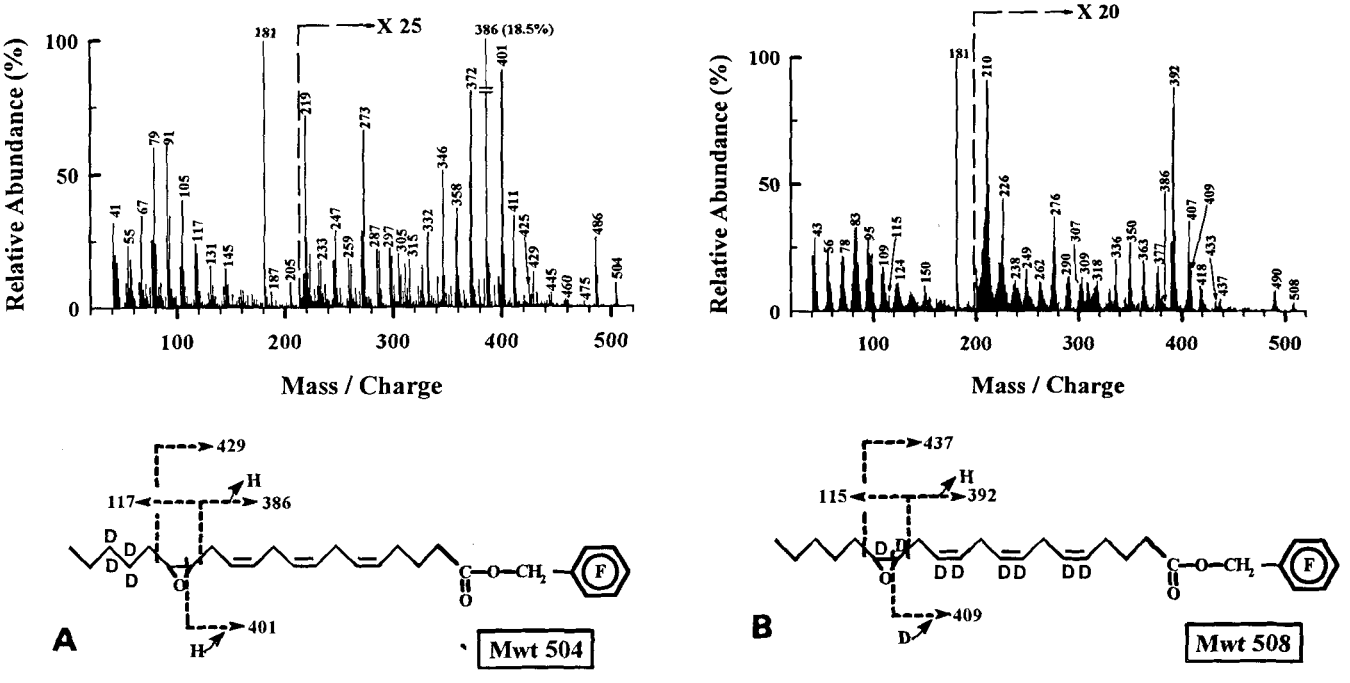

Fig. 5. Electron ionization mass spectra of the pentafluorobenzyl ester of 14,15-EET (A) [17,17,18,18-d_4], and (B) [5,6,8,9,11,12,14,15-d_8] isotopes.

1.5%), 482 (M-H_2O; 0.5-1.2%), 332 (M-[C_6F_5+H]; 0.0-1.9%) and 301 (M-[$C_6F_5CH_2$+H_2O]; 1.4-2.9%). However, in contrast to the NICI spectra, the electron ionization spectra indicated the position of the oxirane ring. Fragments in the 14,15-EET spectrum indicated cleavages α to the oxirane ring: 429 (M-$CH_3(CH_2)_4$), 411 (M-[$CH_3(CH_2)_4$+H_2O]), 386 (M-$CH_3(CH_2)_4CH(O)CH_2$), and 113 ($CH_3(CH_2)_4CH(O)CH$) (Fig. 4A). Other fragments indicated transannular cleavages: 401 (M-$CH_3(CH_2)_4CO$) and 99 ($CH_3(CH_2)_4CO$) (21, 22). Comparable ions in the spectra of the other EET regioisomers similarly suggested alpha and transannular cleavages, and thus oxirane ring positions: 11,12-EET: 389 (M-$CH_3(CH_2)_4CH{=}CHCH_2$), 361 ([CH_2]$_2$[$CH{=}CHCH_2$]$_2$(CH_2)$_3$$COOCH_2C_6F_5$), 346 (CH[$CH{=}CHCH_2$]$_2$-($CH_2$)$_3$$COOCH_2C_6F_5$), and 153 ($CH_3(CH_2)_4CH{=}CHCH_2$-$CH(O)CH$) (Fig. 4B); 8,9-EET: 349 (M-$CH_3(CH_2)_4$-[$CH{=}CHCH_2$]$_2$), 337 (M-$CH_3(CH_2)_4$[$CH{=}CHCH_2$]$_2$C), 193 ($CH_3(CH_2)_4$[$CH{=}CHCH_2$]$_2$$CH(O)CH$) and 150 ($CH_3(CH_2)_4CH{=}CHCH_2CH{=}CHCH$) (Fig. 4C); and 5,6-EET: 309 (M-$CH_3(CH_2)_4$[$CH{=}CHCH_2$]$_3$), 297 (M-$CH_3(CH_2)_4$[$CH{=}CHCH_2$]$_3$C), 281 (M-$CH_3(CH_2)_4$-[$CH{=}CHCH_2$]$_3$CO), 233 ($CH_3(CH_2)_4$[$CH{=}CHCH_2$]$_3$-$CH(O)CH$), 219 ($CH_3(CH_2)_4$[$CH{=}CHCH_2$]$_3$CO), 203 ($CH_3(CH_2)_4$[$CH{=}CHCH_2$]$_3$C) and 190 ($CH_3(CH_2)_4$-[$CH{=}CHCH_2$]$_2$$CH{=}CHCH$), respectively (Fig. 4D). Due to these cleavages, the electron ionization spectra were diagnostic and readily differentiated between the

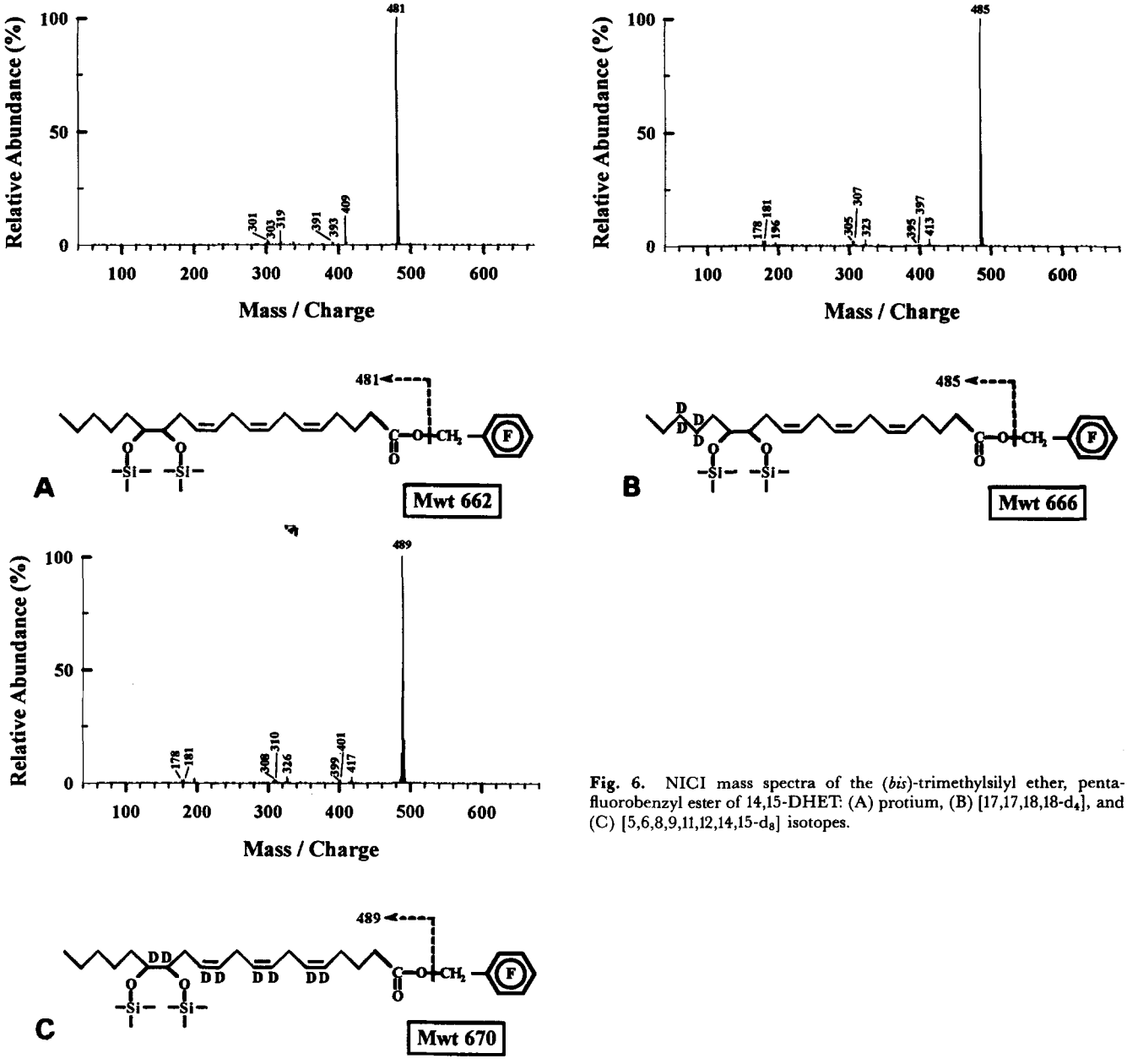

Fig. 6. NICI mass spectra of the (*bis*)-trimethylsilyl ether, pentafluorobenzyl ester of 14,15-DHET: (A) protium, (B) [17,17,18,18-d_4], and (C) [5,6,8,9,11,12,14,15-d_8] isotopes.

EET standards. However, it should be emphasized that when biological samples are analyzed, some of the diagnostic ions that occur in low intensity may not be readily detectable due to matrix contributions.

To validate the above interpretations (which were based on spectra derived from methyl and picolinyl esters, as reviewed in ref. 7), deuterated EETs were synthesized, converted to pentafluorobenzyl esters, and similarly analyzed. In the spectrum of 14,15-EET[17,17,18,18-d_4], *m/z* 500, 482, 301, and 99 increased by four daltons, but *m/z* 429, 411, 401, and 386 did not increase in size (Fig. 4A vs. **Fig. 5A**). In the spectrum of 14,15-EET[5,6,8,9,11,12,14,15-d_8], *m/z* 500, 482, 429, and 401 ions increased by eight daltons while *m/z* 411, 386, 332,

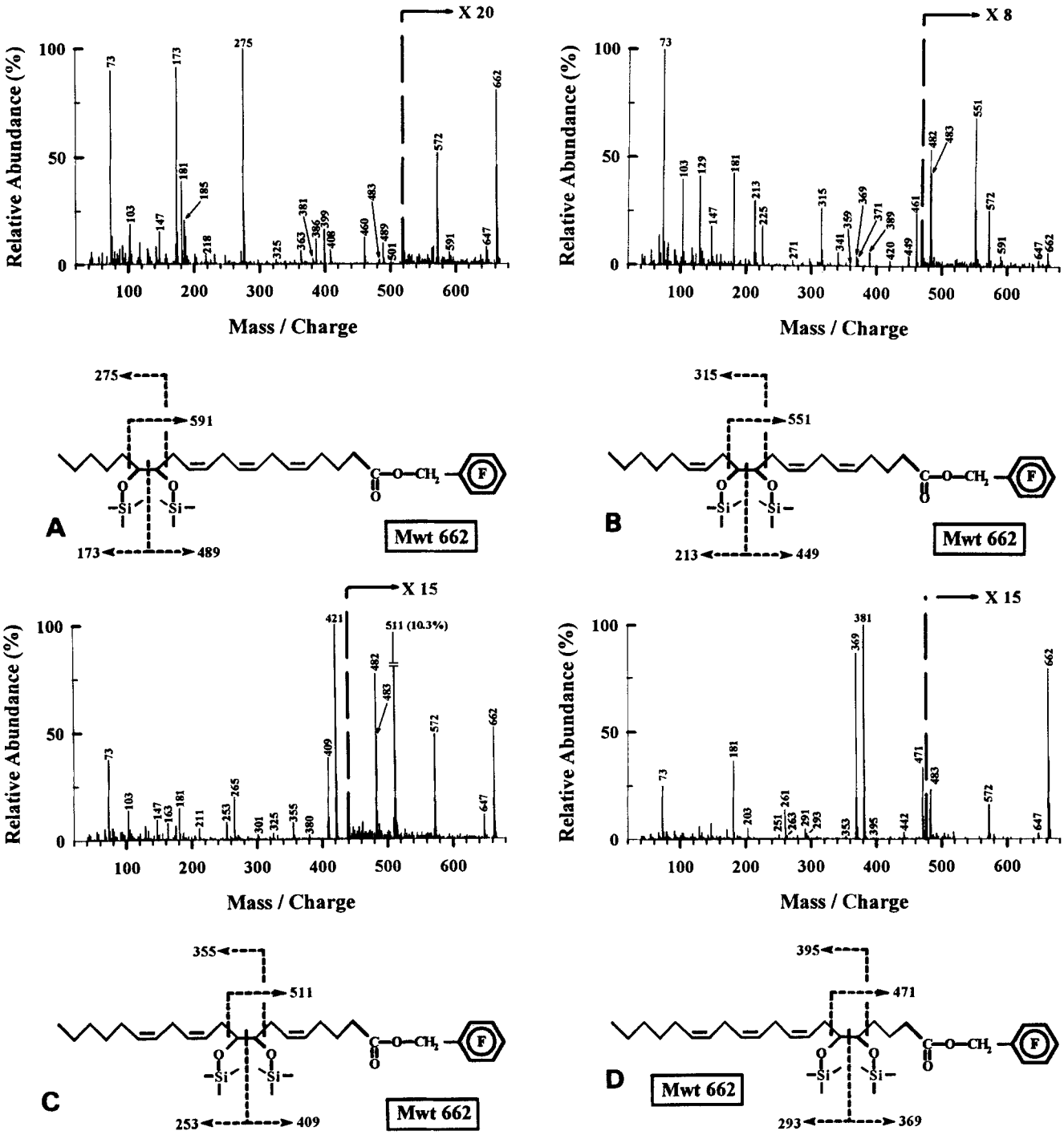

Fig. 7. Electron ionization mass spectra of the (*bis*)-trimethylsilyl ether, pentafluorobenzyl ester of (A) 14,15-, (B) 11,12-, (C) 8,9-, and (D) 5,6-DHET.

and 301 increased to 418, 392, 336, and 307, respectively; *m/z* 99 remained unaltered (Fig. 4A vs. Fig. 5B). In addition to confirming the molecular weights, the ion shifts documented that *m/z* 429, 411, 401, 386, and 113 characterized the position of the oxirane ring. Moreover, spectra of the d_8 standards demonstrated that not all hydrogen atoms in the water losses came from the oxirane ring carbons: 418 = 508 − [$CH_3(CH_2)_4$ + HOD], 419 = 508 − [$CH_3(CH_2)_4$ + H_2O]. Comparable results were obtained when deuterated standards of the other three EET regioisomers were also examined (data not shown). Thus, the electron ionization spectra of EET pentafluorobenzyl esters contained fragments that identified the oxirane position, and may, depending upon the contributions from the biological matrix, be used to differentiate between isomers. Moreover, 40 ng of each EET was enough to generate a full electron ionization spectrum; the corresponding signal-to-noise ratio was 126 ± 12 to 1.0 for the four regioisomers.

NICI spectra of (*bis*) trimethylsilyl ether-DHET-PFB

Two hundred fifty pg of each DHET was enough to generate a representative spectrum; under these circumstances, the signal-to-noise ratio for the corresponding total ion current averaged 20 to 1 for the regioisomers. As shown for 14,15-DHET (**Fig. 6A**), each DHET spectrum contained *m/z* 481 (M-$CH_2C_6F_5$, 100%), 409 (M-[$CH_2C_6F_5$ + CH_2=$Si(CH_3)_2$]; 4.8–8.8%), 393 (M-[$OCH_2C_6F_5$ + CH_2=$Si(CH_3)_2$]; 0.2–0.5%), 391 (M-[$CH_2C_6F_5$ + $HOSi(CH_3)_3$]; 0.1–0.2%), 319 (M-[$CH_2C_6F_5$ + CH_2=$Si(CH_3)_2$ + $HOSi(CH_3)_3$]; 1.6–4.7%), 303 (M-[$OCH_2C_6F_5$ + CH_2=$Si(CH_3)_2$ + $HOSi(CH_3)_3$]; 0.9–1.9%), and 301 (M-[$CH_2C_6F_5$ + 2×$HOSi(CH_3)_3$]; 1.1–2.0%). In contrast to previous results (6), the present spectral interpretations were validated using synthetic, deuterated DHET standards. In the spectrum of 14,15-DHET[17,17,18,18-d_4], the masses of the fragments all increased by 4 daltons (Fig. 6B), suggesting that these fragments do not lose carbons from the methyl end. Likewise, in the spectrum of 14,15-DHET[5,6,8,9,11,12,14,15-d_8], fragments 481, 409, 393 increased by 8 daltons (Fig. 6C), and indicated that they possessed an intact carbon skeleton. In contrast, *m/z* 391, 319, 303, and 301 increased by both 7 and 8 daltons, and documented that deuterium atoms from C_{14} and C_{15}, as well as protium atoms from non-contiguous carbons, were lost as $DOSi(CH_3)_3$ and $HOSi(CH_3)_3$, respectively. Comparable patterns of mass shifts were noted when spectra from the three other DHET regioisomers were examined (data not shown). Thus, in addition to the base peak *m/z* 481, multiple minor fragments in the NICI spectra confirmed the molecular weight of 662. When only *m/z* 481 was monitored, 5.0 fg DHET was enough to generate a detectable peak with a signal-to-noise ratio of 15 to 1.0. Thus, 5.0 fg of the (*bis*)trimethylsilyl ether, pentafluorobenzyl ester derivative was sufficient to establish a DHET molecular weight of 662.

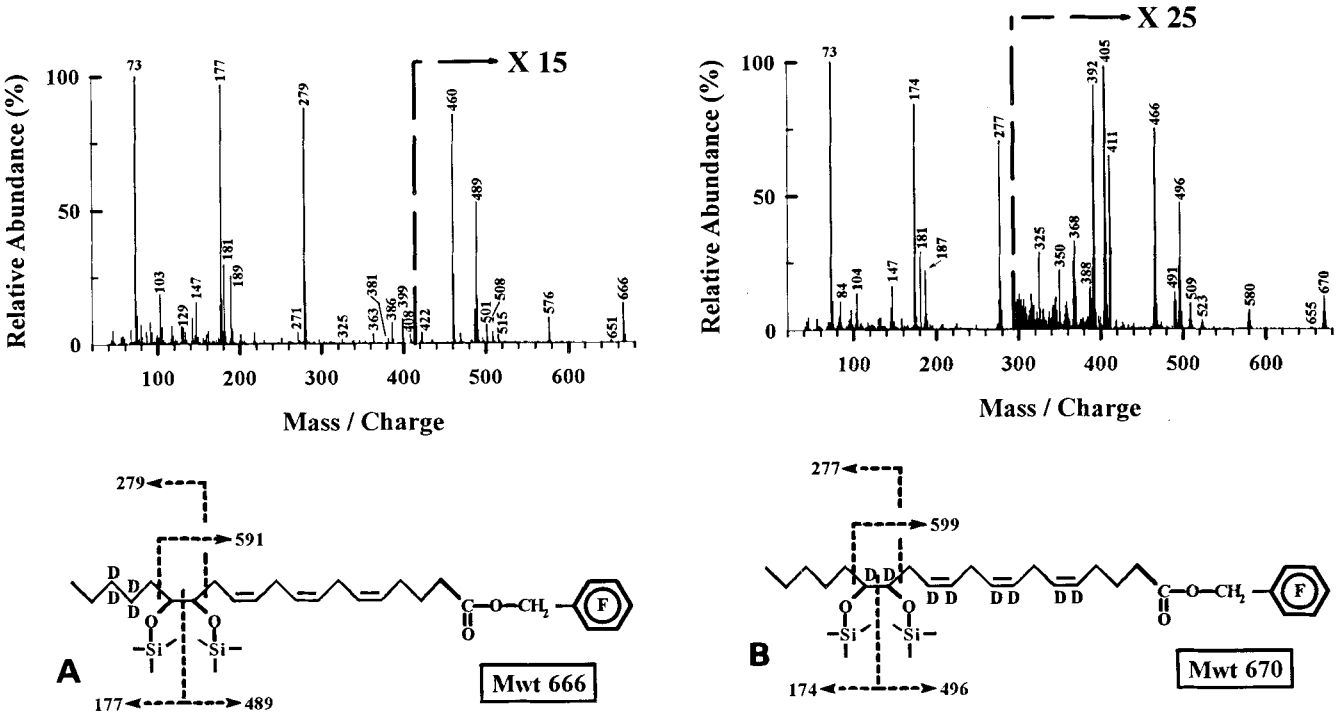

Fig. 8. Electron ionization mass spectra of the (*bis*)-trimethylsilyl ether, pentafluorobenzyl ester of 14,15-DHET (A) [17,17,18,18-d_4], and (B) [5,6,8,9,11,12,14,15-d_8] isotopes.

Electron ionization spectra of (*bis*) trimethylsilyl ether-DHET-PFB

Fifteen ng of each DHET generated a representative electron ionization spectrum that was associated with a total ion current signal-to-noise ratio of 260 to 1.0. In contrast to NICI spectra, the electron ionization spectra were diagnostic and this derivative permitted differentiation of the regioisomers (**Fig. 7**). As found for the NICI spectra, the electron ionization spectra revealed a molecular weight of 662 for all four regioisomers: 662 (M), 647 (M-CH_3), 572 (M-$(CH_3)_3SiOH$), and 483 (M-C_7F_5). In addition, the electron ionization spectra contained ions that reflected cleavages α to the trimethylsilyl ether groups. Thus, in the spectrum of 14,15-DHET, the positions of the trimethylsilyl ether groups were indicated by *m/z* 591 (M-$CH_3(CH_2)_4$), 501 (M-[$CH_3(CH_2)_4$ + $HOSi(CH_3)_3$]), 489 (M-$CH_3(CH_2)_4CHOSi(CH_3)_3$), 460 (M-$CH_3(CH_2)_4CHOSi(CH_3)_3CHO$), 399 (M-[$CH_3(CH_2)_4$-$CHOSi(CH_3)_3$ + $HOSi(CH_3)_3$]), 386 (M-[$CH_3(CH_2)_4$-[$CHOSi(CH_3)_3]_2$ + H]]), 381 (M-[$CH_3(CH_2)_4CHO$ + $CH_2C_6F_5$]), 275 ($CH_3(CH_2)_4[CHOSi(CH_3)_3]_2$), 185 ($CH_3$-$(CH_2)_4[CHOSi(CH_3)_3]_2$-$HOSi(CH_3)_3$)) and 173 ($CH_3$-$(CH_2)_4CHOSi(CH_3)_3$) (Fig. 7A). The *m/z* 460 and 381 fragments may have reflected cleavages following the migration of a $(CH_3)_3Si$ moiety to the carbonyl oxygen based on studies involving (*bis*)-trimethylsilyl ether, methyl esters (see references in ref. 12). The trimethylsilyl ethers

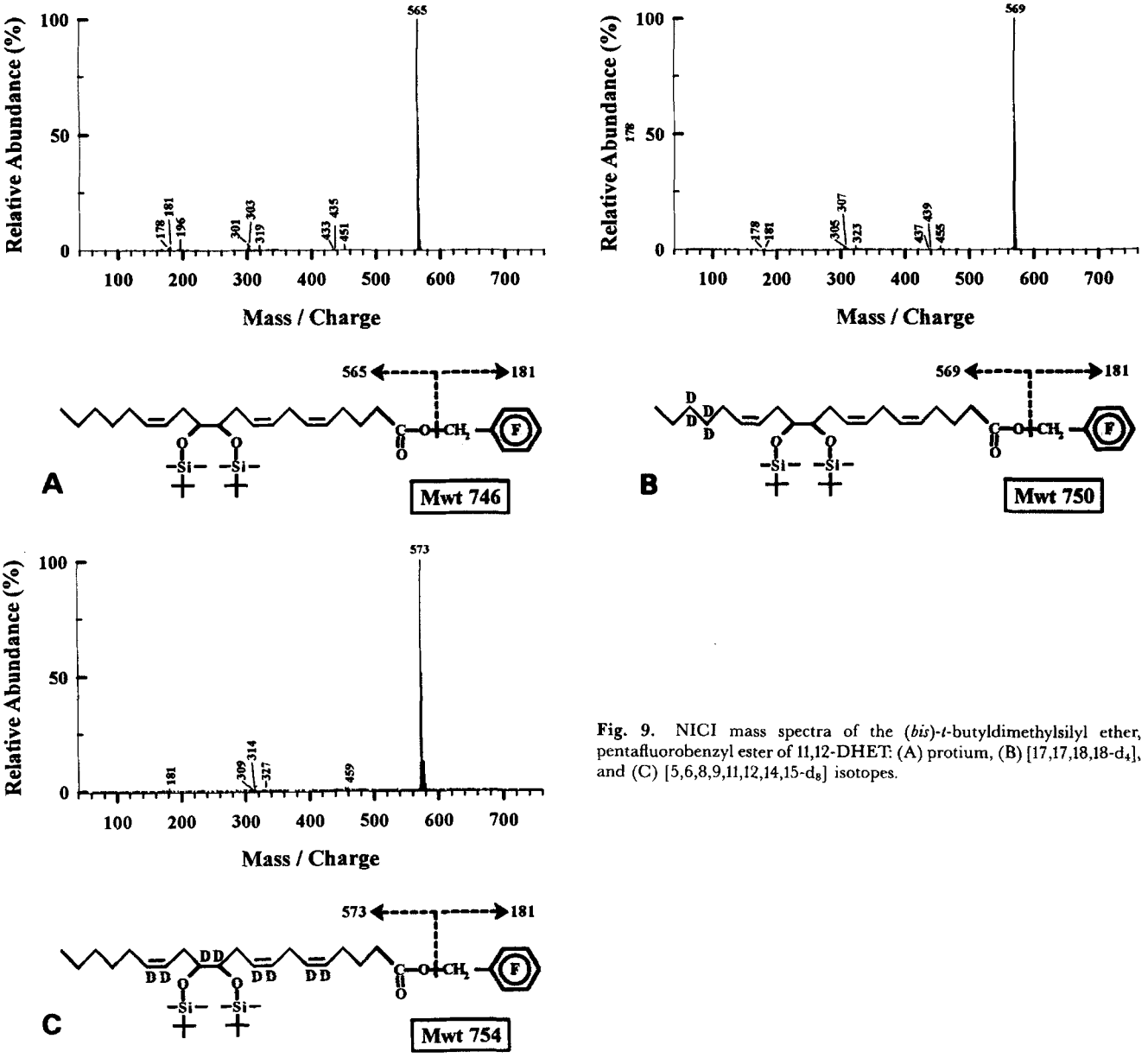

Fig. 9. NICI mass spectra of the (*bis*)-*t*-butyldimethylsilyl ether, pentafluorobenzyl ester of 11,12-DHET: (A) protium, (B) [17,17,18,18-d_4], and (C) [5,6,8,9,11,12,14,15-d_8] isotopes.

also directed electron-induced cleavages for pentafluorobenzyl esters of the other EET regioisomers, and therefore facilitated the identification of the original (*vic*)diol position: 11,12-DHET: 551 (M-$CH_3(CH_2)_4CH{=}CHCH_2$), 461 (M-[$CH_3(CH_2)_4CH{=}CHCH_2$+$HOSi(CH_3)_3$]), 449 (M-$CH_3(CH_2)_4CH{=}CHCH_2CHOSi(CH_3)_3$), 420 (M-$CH_3(CH_2)_4CH{=}CHCH_2CHOSi(CH_3)_3CHO$), 371 (M-[$CH_3(CH_2)_4CH{=}CHCH_2$ + 2× $HOSi(CH_3)_3$]), 359 ($C[CH_2CH{=}CH]_2(CH_2)_3COOC_6F_5$), 315 ($CH_3(CH_2)_4$-$CH{=}CHCH_2[CHOSi(CH_3)_3]_2$), 225 ($CH_3(CH_2)_4CH{=}$ $CHCH_2CHOSi(CH_3)_3C$), and 213 ($CH_3(CH_2)_4CH{=}$ $CHCH_2CHOSi(CH_3)_3$) (Fig. 7B); 8,9-DHET: 511 (M-$CH_3(CH_2)_4[CH{=}CHCH_2]_2$), 482 (M-$CH_3(CH_2)_4[CH{=}$ $CHCH_2]_2CHO$), 421 (M-[$CH_3(CH_2)_4[CH{=}CHCH_2]_2$+

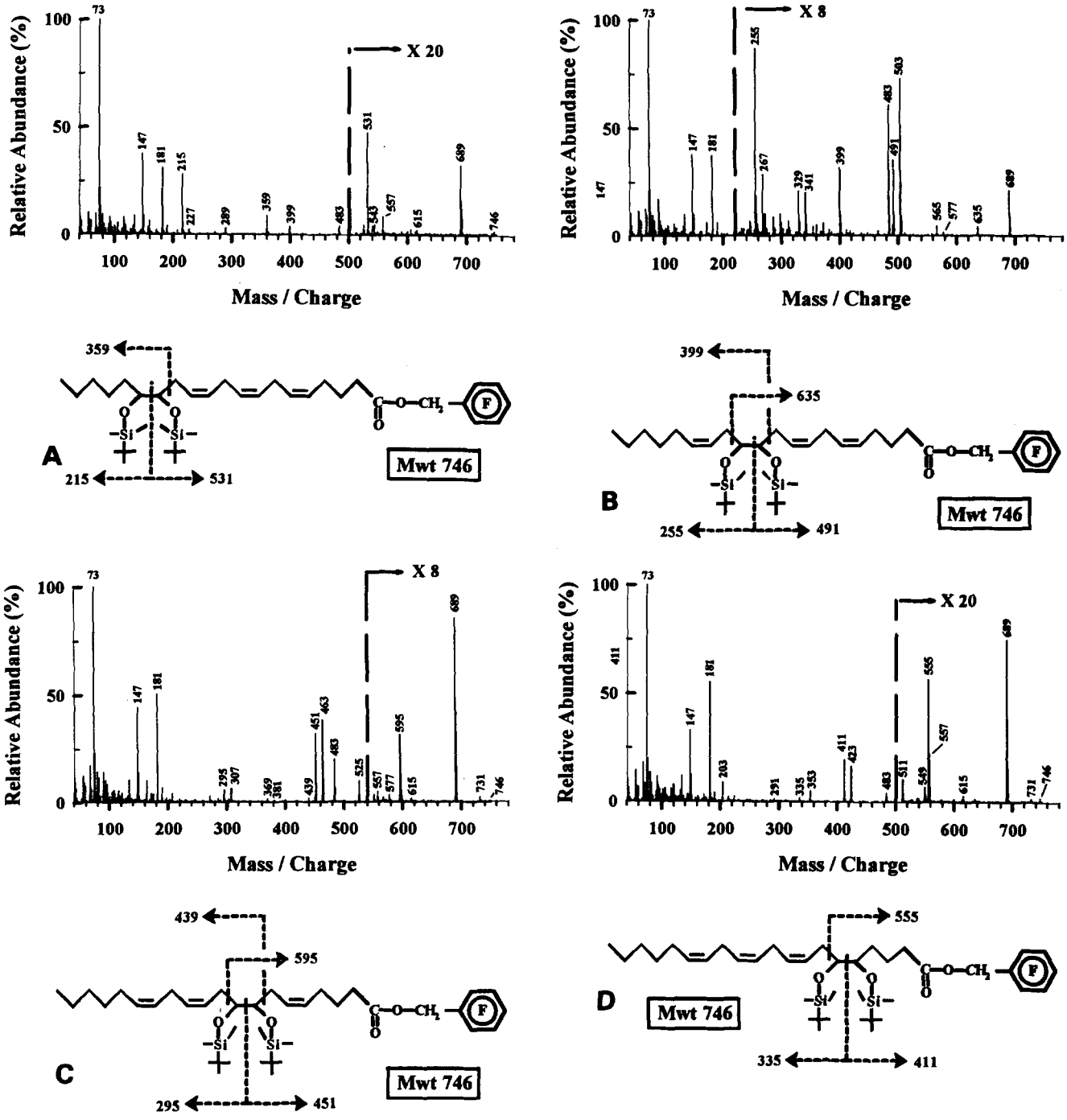

Fig. 10. Electron ionization mass spectra of the (*bis*)-*t*-butyldimethylsilyl ether, pentafluorobenzyl ester of (A) 14,15-, (B) 11,12-, (C) 8,9-, and (D) 5,6-DHET.

$HOSi(CH_3)_3]$), 409 ($CHOSi(CH_3)_3CH_2CH{=}CH(CH_2)_3COOCH_2C_6F_5$), 380 ($CH_2CH{=}CH(CH_2)_3COSi(CH_3)_3OCH_2C_6F_5$), 355 ($M{-}CH_2CH{=}CH(CH_2)_3COOCH_2C_6F_5$), 265 ($M{-}[CH_2CH{=}CH(CH_2)_3COOCH_2C_6F_5 + HOSi(CH_3)_3]$), 253 ($CH_3(CH_2)_4[CH{=}CHCH_2]_2CHOSi(CH_3)_3$), and 163 ($CH_3(CH_2)_4[CH{=}CHCH_2]_2C$) (Fig. 7C); and 5,6-DHET: 471 ($M{-}CH_3(CH_2)_4[CH{=}CHCH_2]_3$), 442 ($CHOSi(CH_3)_3(CH_2)_3COSi(CH_3)_3OCH_2C_6F_5$), 395 ($CH_3(CH_2)_4[CH{=}CHCH_2]_3[CHOSi(CH_3)_3]_2$), 381 ($M{-}[CH_3(CH_2)_4[CH{=}CHCH_2]_3 + HOSi(CH_3)_3]$), 369 ($CHOSi(CH_3)_3(CH_2)_3COOCH_2C_6F_5$), 293 ($CH_3(CH_2)_4[CH{=}CHCH_2]_3CHOSi(CH_3)_3$), and 279 ($C(CH_2)_3COOCH_2C_6F_5$) (Fig. 7D), respectively. Thus, the electron ionization spectra of (*bis*)trimethylsilyl ether, pentafluorobenzyl esters of DHETs were diagnostic for the individual regioisomers.

Synthetic, deuterated DHET standards were used to validate the interpretations of the electron ionization spectra. In the spectrum of 14,15-DHET[17,17,18,18-d_4], *m/z* 662, 647, 572, 483, 275, 185, and 173 increased by 4 daltons, while *m/z* 591, 501, 489, 460, 399, and 381 did not increase in size (Fig. 7A vs. **Fig. 8A**). In the spectrum of 14,15-DHET[5,6,8,9,11,12,14,15-d_8], *m/z* 662, 647, 591, 572, 501, and 483 increased by 8 daltons, while *m/z* 489, 460, 399, 381, 275, 185, and 173 increased only to 496 ($M{-}CH_3(CH_2)_4CDOSi(CH_3)_3$), 466 ($M{-}CH_3(CH_2)_4CDOSi(CH_3)_3CDO$), 405 ($M{-}[CH_3(CH_2)_4CDOSi(CH_3)_3 + DOSi(CH_3)_3]$), 388 ($M{-}[CH_3(CH_2)_4CDO + CH_2C_6F_5]$), 277 ($CH_3(CH_2)_4[CDOSi(CH_3)_3]_2$), 187 ($CH_3(CH_2)_4[CDOSi(CH_3)_3]_2{-}HOSi(CH_3)_3$), and 174 ($CH_3(CH_2)_4CDOSi(CH_3)_3$), respectively (Fig. 7A vs. Fig. 8B). The mass shifts confirmed the above interpretations and established that fragments 591, 501, 489, 460, 399, 381, 275, 185, and 173 identified the $C_{14}C_{15}$ diol position. Comparable mass shift patterns were noted when the three other DHET regioisomers were studied (data not shown). Thus, pentafluorobenzyl esters when analyzed in the electron ionization mode established both the molecular weight of DHETs and the position of the vicinal diol.

NICI spectra of (*bis*)-*t*-butyldimethylsilyl ether-DHET-PFB

An injection of 420 pg of DHET was adequate to generate a representative NICI spectrum, which was associated with a total ion current signal-to-noise of 14 to 1.0. As illustrated for 11,12-DHET in **Fig. 9A,** the spectra of DHETs contained the following *m/z* in common: 565 ($M{-}CH_2C_6F_5$; 100%), 451 ($M{-}[CH_2C_6F_5 + 2\times C(CH_3)_3]$; 2.2–3.2%), 435 ($M{-}[CC_6F_5 + HOSi(CH_3)_2C(CH_3)_3]$, 0.2–0.4%); 433 ($M{-}[CH_2C_6F_5 + HOSi(CH_3)_2C(CH_3)_3]$; 0.3–0.7%), 319 ($M{-}[CH_2C_6F_5 + HOSi(CH_3)_2C(CH_3)_3 + (CH_3)_3CSi(CH_3){=}CH_2]$; 2.3–4.6%), 303 ($M{-}[OCH_2C_6F_5 + HOSi(CH_3)_2C(CH_3)_3 + (CH_3)_3CSi(CH_3){=}CH_2]$; 1.5–2.1%), and 301 ($M{-}[CH_2C_6F_5 + 2\times HOSi(CH_3)_2C(CH_3)_3]$; 2.2–3.2%). The NICI spectral interpretations were validated using synthetic, deuterated DHET standards. In the spectrum of

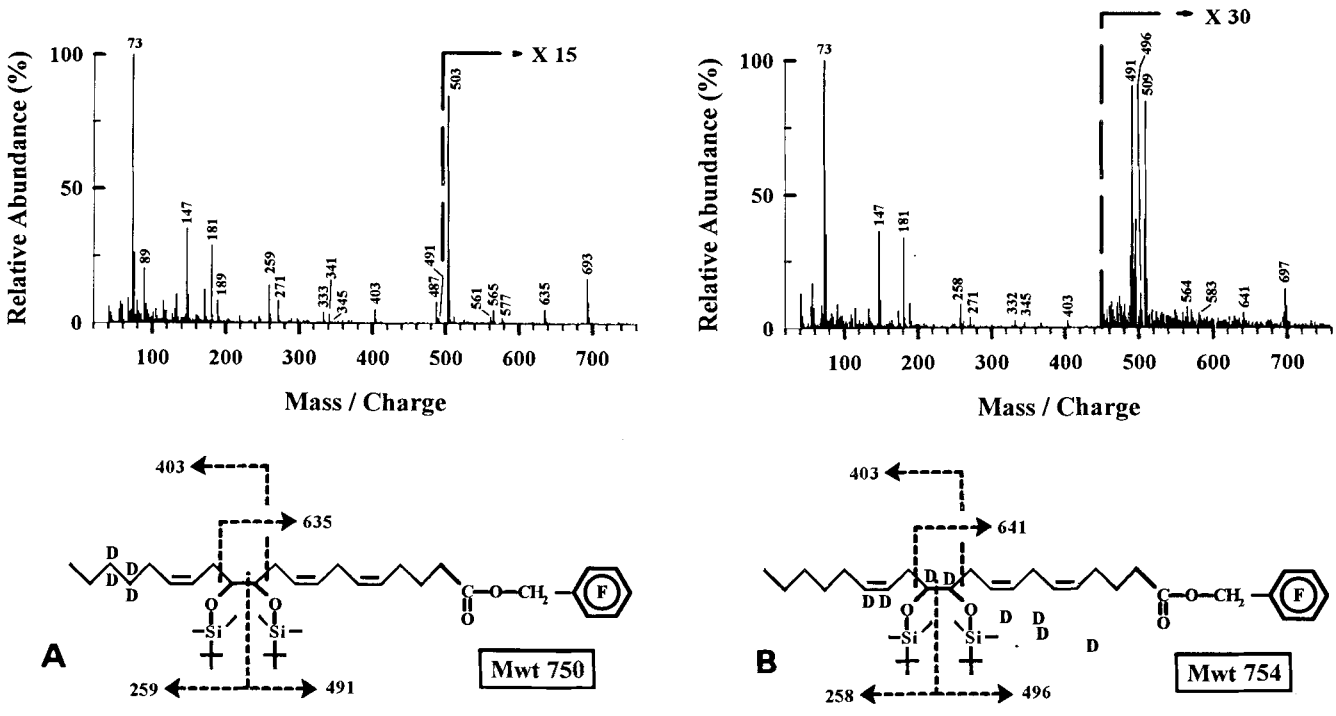

Fig. 11. Electron ionization mass spectra of the (*bis*)-*t*-butyldimethylsilyl ether, pentafluorobenzyl ester of 11,12-DHET (A) [17,17,18,18-d_4], and (B) [5,6,8,9,11,12,14,15-d_8] isotopes.

11,12-DHET[17,17,18,18 d_4], the mass of each of the above fragments increased by 4 daltons (Fig. 9B), suggesting that they did not lose C_{17} and C_{18} with attached deuterium atoms. Similarly, fragments 565, 451, and 319 increased by 8 daltons in the spectrum of 11,12-DHET[5,6,8,9,11,12,14,15-d_8] (Fig. 9C), and indicated that these fragments essentially retained the original carbon skeleton. In contrast, the weaker *m/z* 435, 433, 303, and 301 increased by both 7 and 8 daltons, and suggested that deuterium atoms from C_{11} and C_{12}, as well as protium atoms from noncontiguous carbons, may have been lost as $DOSi(CH_3)_2C(CH_3)_3$ and $HOSi(CH_3)_2C(CH_3)_3$, respectively (Fig. 9C). Similar mass shift patterns were noted in the spectra of the other DHET regioisomers (data not shown). Thus, in addition to the base peak *m/z* 565, the minor fragments in each NICI spectrum confirmed the 746 molecular weight. When only *m/z* 565 was continuously and selectively monitored, 50 fg (*bis*)-*t*-butyldimethylsilyl ether, pentafluorobenzyl ester DHET was adequate to establish the molecular weight of each DHET with a signal-to-noise ratio of 92 to 1.0. Nevertheless, none of the NICI spectra differentiated between the four DHET regioisomers. However, because up to 80 pg of each DHET regioisomer was well resolved by capillary GC (Fig. 1), fg to pg quantities of individual DHETs could therefore be identified by capillary gas chromatography and mass spectrometry in the NICI mode.

Electron ionization spectra of (*bis*)-*t*-butyldimethylsilyl ether-DHET-PFB

Twenty three ng of each DHET was enough to generate a full electron ionization spectrum (**Fig. 10**) that corresponded to a total ion current signal-to-noise of 115 to 1.0. As with the NICI spectra, the electron ionization spectra contained ions that indicated a molecular weight of 746: 746 (M; 0.0–0.1%), 689 ($M-C(CH_3)_3$; 1.6–10.5%), 615 ($M-OSi(CH_3)_2C(CH_3)_3$; 0.0–0.3 %), 557 ($M-[C(CH_3)_3+HOSi(CH_3)_2C(CH_3)_3]$; 0.0–0.6%), and 483 ($M-[HOSi(CH_3)_2C(CH_3)_3+OSi(CH_3)_2C(CH_3)_3]$; 4.1–19.8%). Additional fragments were also present in the electron ionization spectra that reflected α cleavages to *vicinal* *t*-butyldimethylsilylether groups. For example, the spectrum of 14,15-DHET contained *m/z* 543 ($M-[CH_3(CH_2)_4+HOSi(CH_3)_2C(CH_3)_3]$), 531 ($M-CH_3(CH_2)_4CHOSi(CH_3)_2C(CH_3)_3$), 399 ($M-[CH_3(CH_2)_4CHOSi(CH_3)_2C(CH_3)_3+HOSi(CH_3)_2C(CH_3)_3]$), 359 ($CH_3(CH_2)_4[CHOSi(CH_3)_2C(CH_3)_3]_2$), 227 ($CH_3(CH_2)_4[CHOSi(CH_3)_2C(CH_3)_3]_2-HOSi(CH_3)_2C(CH_3)_3$), and 215 ($CH_3(CH_2)_4CHOSi(CH_3)_2C(CH_3)_3$) (Fig. 10A). The spectrum of 11,12-DHET contained *m/z* 635 ($M-CH_3(CH_2)_4CH=CHCH_2$); 577 ($M-[CH_3(CH_2)_4CH=CHCH_2+HC(CH_3)_3]$); 503 ($M-[CH_3(CH_2)_4CH=CHCH_2+HOSi(CH_3)_2C(CH_3)_3]$), 491 ($M-CH_3(CH_2)_4CH=CHCH_2CHOSi(CH_3)_2C(CH_3)_3$), 399 ($CH_3(CH_2)_4CH=CHCH_2[CHOSi(CH_3)_2C(CH_3)_3]_2$), 341 ($CHCH=CHCH_2[CHOSi(CH_3)_2C(CH_3)_3]_2$), 267 ($CH_3-(CH_2)_4CH=CHCH_2CHCHOSi(CH_3)_2C(CH_3)_3CH$), and 255 ($CH_3(CH_2)_4CH=CHCH_2CHOSi(CH_3)_2C(CH_3)_3$) (Fig. 10B). The spectrum of 8,9-DHET contained the diagnostic *m/z* 595 ($M-CH_3(CH_2)_4[CH=CHCH_2]_2$), 463 ($M-[CH_3-(CH_2)_4[CH=CHCH_2]_2+HO(CH_3)_2SiC(CH_3)_3]$), 451 ($M-CH_3(CH_2)_4[CH=CHCH_2]_2CHOSi(CH_3)_2C(CH_3)_3$), 439 ($M-CH_3(CH_2)_4[CH=CHCH_2]_2[CHOSi(CH_3)_2C(CH_3)_3]_2$), 381 ($CH_3(CH_2)_4[CH=CHCH_2]_2[CHOSi(CH_3)_2C(CH_3)_3]_2-HC(CH_3)_3$), 307 ($CH_3(CH_2)_4[CH=CHCH_2]_2[CHOSi(CH_3)_2-C(CH_3)_3]_2-HO(CH_3)_2SiC(CH_3)_3$), and 295 ($CH_3(CH_2)_4-[CH=CHCH_2]_2CHOSi(CH_3)_2C(CH_3)_3$) (Fig. 10C). Finally, the spectrum of 5,6-DHET contained *m/z* 555 ($[CHOSi(CH_3)_2C(CH_3)_3]_2(CH_2)_3COOCH_2C_6F_5$), 423 ($[CHOSi(CH_3)_2C(CH_3)_3]_2(CH_2)_3COOCH_2C_6F_5-HOSi(CH_3)_2-C(CH_3)_3$), 411 ($CHOSi(CH_3)_2C(CH_3)_3(CH_2)_3COOCH_2-C_6F_5$), 353 ($CHOSi(CH_3)_2C(CH_3)_3(CH_2)_3COOCH_2-C_6F_5-HC(CH_3)_3$), 335 ($CH_3(CH_2)_4[CH=CHCH_2]_3-CHOSi(CH_3)_2C(CH_3)_3$), 291 ($[CHOSi(CH_3)_2C(CH_3)_3]_2(CH_2)_3COOCH_2C_6F_5-2\times HOSi(CH_3)_2C(CH_3)_3$), and 203 ($CH_3(CH_2)_4[CH=CHCH_2]_3CHOSi(CH_3)_2C(CH_3)_3-HOSi(CH_3)_2C(CH_3)_3$) (Fig. 10D). Thus, analogous to the trimethylsilylethers, the *t*-butyldimethylsilyl ethers directed electron-induced cleavages for the pentafluorobenzyl esters and generated diagnostic spectra of individual DHETs.

Deuterated standards were used to validate the interpretations of the electron ionization spectra of the *t*-butyldimethylsilyl ether derivatives. In the spectrum of 11,12DHET[17,17,18,18-d_4], *m/z* 689, 557, 483, 399, 341, 267, and 255 increased by 4 daltons while *m/z* 635, 577, 503, 491, 181 ($C_6F_5CH_2$), 147 ($CH_2=Si(CH_3)OSi(CH_2)-(CH_3)OH$) and 73 ($OSi(CH_3)=CH_2$) did not increase in size (Fig. 10B vs. **Fig. 11A**). As expected from the spectral interpretations, those fragments that increased by 4 daltons contained C_{17} and C_{18}, whereas fragments without mass increases did not contain these carbons and their attached deuterium atoms. In the spectrum of 11,12-EET[5,6,8,9,11,12,14,15-d_8], only *m/z* 697 ($M-C(CH_3)C$) and 491 ($M-[OSi(CH_3)_2C(CH_3)_3+HOSi(CH_3)_2C(CH_3)_3]$ showed an 8 dalton increase (Fig. 10B vs. Fig. 11B). However, *m/z* 564 ($M-[C(CH_3)_3+DOSi(CH_3)_2C(CH_3)_3]$ showed a 7 dalton increase, while *m/z* 641 ($M-CH_3(CH_2)_4CD=CDCH_2$), 583 ($M-[CH_3(CH_2)_4CD=CDCH_2+HC(CH_3)_3]$), and 509 ($M-[CH_3(CH_2)_4CD=CDCH_2+HOSi(CH_3)_2-C(CH_3)_3]$) demonstrated a 6 dalton increase. Moreover, *m/z* 496 ($M-CH_3(CH_2)_4CD=CDCH_2CDOSi(CH_3)_2-C(CH_3)_3$) showed a 5 dalton increase, while *m/z* 403 ($CH_3(CH_2)_4CD=CDCH_2[CDOSi(CH_3)_2C(CH_3)_3]_2$, 345 ($CHCD=CDCH_2[CDOSi(CH_3)_2C(CH_3)_3]_2$, and 271 ($CH_3(CH_2)_4CD=CDCHCDOSi(CH_3)_2C(CH_3)_3CD$) or *m/z* 258 ($CH_3(CH_2)_4CD=CDCH_2CDOSi(CH_3)_2C(CH_3)_3$) demonstrated 4 or 3 dalton mass increases, respectively. The predictability of the above mass shifts validated our interpretations of the non-deuterated compounds. Thus, the electron ionization spectra of *t*-butyldimethylsilyl

ether, pentafluorobenzyl esters produced diagnostic and readily interpretable spectra of the four DHET regioisomers. Moreover, DHETs could still be identified by the more conventional electron ionization techniques, even when the necessity for higher (ng) amounts reduced the gas chromatographic resolution of the regioisomers.

In summary, only ng quantities of EET regioisomers as pentafluorobenzyl esters were required for identification by GC–MS when examined in the electron-ionization mode. In contrast to other derivatives, the spectra of the pentafluorobenzyl esters had multiple diagnostic ions in the high mass range with moderate to low intensities. Significantly lesser amounts of EETs (femtogram-to-picogram) could also be identified when EETs were first converted to DHETs and analyzed as (*bis*)-*t*-butyldimethylsilyl ether, pentafluorobenzyl esters. Comparisons with the spectra of standards generated in this report and analysis of the pentafluorobenzyl esters in both positive and negative ion modes during capillary gas chromatography will facilitate the identification of endogenously produced EETs and DHETs.

The authors would like to acknowledge the expert technical assistance of Ms. Chu-Han Li, as well as the use of equipment provided by the Gas Chromatography/Mass Spectrometry facility of the University of Iowa. This work was supported by grants from the American Heart Association (#90012560) and the National Institutes of Health (HL-48877, HL-49264, ES-5605, and RR59). Dr. Knapp is an Established Investigator of the American Heart Association.

Manuscript received 19 April 1993, in revised form 8 November 1994, and in re-revised form 7 December 1994.

REFERENCES

1. Oliw, E. H. 1994. Oxygenation of polyunsaturated fatty acids by cytochrome P450 monooxygenases. *Prog. Lipid Res.* **33:** 329–354.
2. Capdevila, J. H., J. R. Falck, and R. W. Estabrook. 1992. Cytochrome P450 and the arachidonate cascade. *FASEB J.* **6:** 731–736.
3. Karara, A., S. Wei, D. Spady, L. Swift, J. H. Capdevila, and J. R. Falck. 1992. Arachidonic acid epoxygenase: structural characterization and quantification of epoxyeicosatrienoates in plasma. *Biochem. Biophys. Res. Commun.* **182:** 1320–1325.
4. Karara, A., E. Dishman, J. R. Falck, and J. H. Capdevila. 1991. Endogenous epoxyeicosatrienoyl-phospholipids. A novel class of cellular glycerolipids containing epoxidized arachidonate moieties. *J. Biol. Chem.* **266:** 7561–7569.
5. Blair, I. A. 1990. Electron-capture negative-ion chemical ionization mass spectrometry of lipid mediators. *Methods Enzymol.* **187:** 13–23.
6. Turk, J., W. T. Stump, W. Conrad-Kessel, R. R. Seabold, and B. A. Wolf. 1990. Quantitation of epoxy- and dihydroxyeicosatrienoic acids by stable isotope-dilution mass spectrometry. *Methods Enzymol.* **187:** 175–186.
7. VanRollins, M., P. D. Frade, and O. A. Carretero. 1989. Synthesis of epoxide and vicinal diol regioisomers from docosahexaenoate methyl esters. *J. Lipid Res.* **30:** 275–286.
8. VanRollins, M. 1990. Synthesis and characterization of cytochrome P-450 epoxygenase metabolites of eicosapentaenoic acid. *Lipids.* **25:** 481–490.
9. Oliw, E. H., F. P. Guengerich, and J. A. Oates. 1982. Oxygenation of arachidonic acid by hepatic monooxygenases. Isolation and metabolism of four epoxide intermediates. *J. Biol. Chem.* **257:** 3771–3781.
10. Keough, T., E. D. Mihelich, and D. J. Eickhoff. 1984. Differentiation of monoepoxide isomers of polyunsaturated fatty acids and fatty acid esters by low-energy charge exchange mass spectrometry. *Anal. Chem.* **56:** 1849–1852.
11. Balazy, M., and A. S. Nies. 1989. Characterization of epoxides of polyunsaturated fatty acids by mass spectrometry via 3-pyridinylmethyl esters. *Biomed. Environ. Mass Spectrom.* **18:** 328–336.
12. VanRollins, M., and R. C. Murphy. 1984. Autooxidation of docosahexaenoic acid: analysis of ten isomers of hydroxydocosahexaenoate. *J. Lipid Res.* **25:** 507–517.
13. Green, K., M. Hamberg, B. Samuelsson, M. Smigel, and J. C. Frolich. 1978. Measurement of prostaglandins, thromboxanes, prostacyclin and their metabolites by gas liquid chromatography–mass spectrometry. *Adv. Prostaglandin Thromboxane Res.* **5:** 39–94.
14. Steffenrud, S., P. Borgeat, M. J. Evans, and M. J. Bertrand. 1987. Mass spectrometric evaluation of the tert.-butyldimethylsilyl derivatives of monohydroxyeicosatetraenoic acids and leukotrienes. *J. Chromatogr.* **423:** 1–14.
15. Capdevila, J. H., J. R. Falck, E. Dishman, and A. Karara. 1990. Cytochrome P-450 arachidonate oxygenase. *Methods Enzymol.* **187:** 385–394.
16. Pace-Asciak, C. R. 1989. Mass spectra of prostaglandins and related products. *Adv. Prostaglandin Thromboxane Leukotriene Res.* **18:** 1–565.
17. Karara, A., E. Dishman, I. Blair, J. R. Falck, and J. H. Capdevila. 1989. Endogenous epoxyeicosatrienoic acids. Cytochrome P-450 controlled stereoselectivity of the hepatic arachidonic acid epoxygenase. *J. Biol. Chem.* **264:** 19822–19827.
18. Karara, A., E. Dishman, H. Jacobson, J. R. Falck, and J. H. Capdevila. 1990. Arachidonic acid epoxygenase. Stereochemical analysis of the endogenous epoxyeicosatrienoic acids of human kidney cortex. *FEBS Lett.* **268:** 227–230.
19. Katoh, T., K. Takahashi, J. Capdevila, A. Karara, J. R. Falck, H. R. Jacobson, and K. F. Badr. 1991. Glomerular stereospecific synthesis and hemodynamic actions of 8,9-epoxyeicosatrienoic acid in rat kidney. *Am. J. Physiol.* **261:** F578–F586.
20. Boeynaems, J. M., A. R. Brash, J. A. Oates, and W. C. Hubbard. 1980. Preparation and assay of monohydroxyeicosatetraenoic acids. *Anal. Biochem.* **104:** 259–267.
21. Aplin, R. T., and L. Coles. 1967. A simple procedure for localisation of ethylenic bonds by mass spectrometry. *Chem. Commun.* 858–859.
22. Gunstone, F. D., and F. R. Jacobsberg. 1972. Fatty Acids, Part 35. The preparation and properties of the complete series of methyl epoxyoctadecanoates. *Chem. Phys. Lipids.* **9:** 26–34.